Hypersonic separated flows: combining CFD and experiment

Sean Creighton[1] Richard Hillier[1] Samuel Mallinson[2] & Simon Williams[1] *

1 Department of Aeronautics, Imperial College London, London SW7 2AZ, United Kingdom,
2 Silverbrook Research, Balmain, NSW, Australia,
corresponding author, r.hillier@imperial.ac.uk

1st September 2003

Abstract

This papers reviews some of the activities in the Hypersonics group of the Department of Aeronautics at Imperial College. For a considerable time we have directed our work to combine experiment and CFD in as effective a manner as possible. This paper presents various aspects of this activity: careful calibration of the tunnel so that 'true' flow conditions may be used as input to the CFD; use of CFD in the design of experiments; a range of experiments, focussing mainly on flow separation, used to explore the flow physics and to provide benchmark cases for code evaluation.

Introduction

High speed aerodynamics presents a particularly demanding research area, experimentally and computationally, so that there is a special advantage in integrating the two approaches as closely as possible. Measurement of many quantities is difficult or impossible, and model manufacture is expensive and time-consuming. Thus CFD can assist in configuration development, either in terms of the overall geometry or in the detail of the location of expensive and sensitive instrumentation, and can 'probe' flow field areas or flow properties that are not accessible to experiments. This does not require unquestioned belief in the accuracy of CFD modelling, however. CFD faces many problems in efficient and accurate algorithm development/implementation (e.g providing adequate mesh density in sensitive flow areas and time-accurate resolution for unsteady flows) and in the flow physics (e.g. turbulence modelling, transition modelling, reaction modelling etc.) so that experiments should both investigate flow physics and also support code development and evaluation. These 'validation' or 'assessment' or experiment/CFD 'partnership' issues have been the subject of many papers and workshops (e.g. [1, 2, 3]). Because of the progressive expansion in CFD, experiments increasingly need to be designed as 'benchmark' studies to provide specific high quality data against which CFD codes might be assessed. This paper therefore focusses mainly on efforts in our laboratory to combine CFD and experiments for a set of 'building block' investigations. These reflect our specific interests and are directed to boundary layer dominated flows including: 'controlled' studies of the effects of increasingly severe pressure gradient on turbulent boundary layer development; shock-induced separations; cavity flows; imposition of 'controlled' three-dimensionality on separated flows.

*Names listed in alphabetical order

The Computational Method

Most details of the CFD approach are available ([4, 5]), so that only the main points are repeated here. The method uses 'convection-diffusion' splitting, solving the convective (i.e Euler) terms using an explicit second-order upwind Godunov-type solver and evaluating the diffusive (viscous) terms with either centred differencing and implicit time integration, for thin layer Navier Stokes formulation, or Runga-Kutta integration for full Navier Stokes. The resultant solver is second order accurate, in space and time, in smooth regions. An ideal equation of state for nitrogen (the experimental test gas) is used, together with the following formulation ([6]) for the temperature dependence of the molecular viscosity ($kg/m/s$),

$$\mu = \frac{1.418 \times 10^{-6} T^{1/2}}{1 + 116.4 T^{-1} 10^{-5/T}} \qquad (1)$$

Constant Prandtl numbers of 0.72 and 0.9 are used in laminar and turbulent regions respectively and all simulations assume isothermal wall conditions (appropriate for a short-duration facility where temperature changes are small) with a wall temperature $T_w = 293$ K.

The turbulence models that are available in the code are simple, with options of an algebraic eddy viscosity model [7], one-equation variants of the $k-\epsilon$ model [8] and the Launder-Sharma formulation of the two-equation $k-\epsilon$ linear eddy viscosity model [9, 10]. Apart from the one-equation Baldwin-Barth model [11, 12], which seems to require a high initial turbulence 'seeding' level and shows excessive dependence upon mesh resolution, all the remaining models produce comparable predictions for attached boundary layer flows. For CFD design these are probably adequate. For high quality modelling, however, there are probably strong reasons for moving to non-linear eddy viscosity and Reynolds stress transport models (e.g. [13]) though little serious assessment is available for high Mach number flows. Compressibility corrections to turbulence models are a complex issue and are not fully understood (e.g. [14]). The turbulent results are presented here without any compressibility correction, though a test with the Wilcox model [10] produces about a 15% reduction in surface heat transfer for the attached boundary layer.

The wind tunnel and flow calibration

The test facility is a gun tunnel, operating with nitrogen gas at a nominal Mach number of 9 and a total temperature in the range of 1000 K to 1150 K – essentially 'cold hypersonics'. The operating unit Reynolds numbers range approximately from 9 million per metre to 47 million per metre. Model lengths up to a maximum of 0.9 m are possible, so that experiments can range from laminar studies to flows with 'natural' transition and extended lengths of turbulent flow. An earlier tunnel calibration exercise [15] was undertaken to ensure that flow initialisation conditions for the CFD can be specified as precisely as possible and includes the effects of (slight) test section axial gradients and flow angularity. In our tunnel the highest unit Reynolds number test condition produces the severest axial Mach number gradient, an increase of approximately 2.7% over one metre. This corresponds to a 19% fall in static pressure; significant for long models, but easily accommodated in the flow initialisation conditions for CFD modelling. An example of this is shown in figure 1. One of our basic test models, upon which a large number of geometric developments have been made, is a long, hollow body of revolution, 75 mm in (outer) dimater, 850 mm length and 12.5 mm wall thickness. The *internal* leading edge is chamfered to form an attached shock wave. The *internal* flow is simply exhausted downstream (considerable developments were required, however, to ensure that this internal flow could be 'swallowed'. The external flow is the test flow. It can be considered as the axisymmetric equiva-

Table 1: Test section flow conditions for 'Low' and 'High' unit Reynolds number operation

M_∞	dM_∞/dx (%/m)	$P0_\infty$ (bar)	$T0_\infty$ (K)	T_{wall} (K)	$Re_\infty(/metre)$
8.9 (± 0.5%)	0	98 (±2%)	1000 (±4%)	293 (±2%)	9,540,000 (±6%)
8.9 (± 0.5%)	2.7	600 (±2%)	1150 (±4%)	293 (±2%)	47,400,000 (±6%)

lent of a flat plate. Figure 1b shows measured surface pressures, compared with CFD simulations. 'Nominal' conditions assumes uniform flow in the stream; 'probe calibration' uses input stream conditions defined by the extensive probe calibration of the test section. 'Model calibration' recognises that the hollow model could be regarded as a large calibration probe in its own right and data from this is included in the calibration data reduction process. Clearly this means that the CFD is 'destined' to give the correct pressure distribution on the model. Nonetheless, these conditions can be used with confidence as a stream calibration for tests on *other* geometries. The figure also includes CFD modelling for surface heat transfer. In this case the solution includes a *pre-specified* zone for laminar-turbulent transition. This shows as much the effect of tunnel gradient on heat transfer as the likely level of accuracy in the use of current turbulence models to predict *nearly* zero pressure gradient heat transfer. At the lowest unit Reynolds number conditions, used for some laminar cavity flow studies, the test section flow is in effect uniform within calibration accuracy over the model length. Table 1 provides flow and calibration data for the tunnel for these two conditions. The total flow duration is 20 ms, of which about 5 ms is taken as the steady flow window. The data presented here are either surface pressure measurements, using miniature Kulite transducers positioned just below the model surface at the end of short tappings to minimise response times, or thin-film platinum resistance-gauges (on MACOR) for heat transfer measurement with temperature histories reduced digitally using the method due to Cook and Felderman ([16], [17]). The measurement accuracy is assessed as $\pm 4\%$ and $\pm 7\%$ for pressure and heat transfer respectively.

The test problems

To study two-dimensional flow fields we regard it as natural to employ bodies of revolution since it is possible to establish high quality two-dimensional axisymmetric flows whereas *nominally* two-dimensional planar flows are always contaminated to some extent by side constraint effects, especially so once flow separation occurs. Thus our two-dimensional studies have used bodies of revolution and our three-dimensional studies have been based upon some controlled departure from the reference axisymmetric flow. Of course, use of an axisymmetric configuration cannot, by itself, guarantee two-dimensionality. A strong, fixed trailing vortex system – Taylor-Goertler-type vortices – has been shown to form downstream of an axisymmetric rearward-facing step in a supersonic flow [18] and, as we will also note later, it is believed that cellular Taylor-Goertler systems can form in cavity flows [4]. Nevertheless, these features are fundamental aspects of the flow physics, rather than a coincidental, and uncontrolled, consequence of side constraints.

Turbulent boundary layer in adverse pressure gradients

The first test concerns the configuration design for the systematic study of turbulent boundary layers in the presence of a family of adverse pressure gradients of increasing severity, developed for the high unit Reynolds number condition of Table 1. Strictly this is not a flow separation case, in that the design was intended to produce severe adverse pressure gradients up to incipient separation, but it nonetheless very

conveniently shows the linking between CFD and experiment. The reference zero pressure gradient (zpg) boundary layer is generated on the exterior of the long hollow circular cylinder referred to earlier in figure 1. This reference boundary layer is then acted-on by the pressure gradient which, for axisymmetric flows, can be generated either by geometric modification of the centrebody (Type 1 - curved wall device) or by use of an external compression cowl (Type 2) to produce a reflected wave system on the centrebody without significant curvature of the test flow. A similar principle has been used in other studies for concave walls [19] and for reflected wave systems ([20, 21, 22]). As a *minimum* design constraint we would wish to specify the required pressure ratio through the interaction and also the severity and profile of the gradient.

Our main pressure gradient investigation [23] has focussed on Type 2, using an external, concentric pressure gradient cowl positioned around the 'centrebody' of Figure 1. The practical advantage of this configuration, experimentally, is that only one set of instrumentation is required on the centrebody irrespective of the number of cowls tested. The design exercise is difficult, however, because of the remoteness of the cowl from the test surface. We set various design specifications for the target pressure distribution including: rapid 'switch-on' and 'switch-off' of the pressure gradient; development of a family of *constant* adverse pressure gradient designs up to the severest possible without producing flow separation; large overall pressure ratios. These were explored by CFD to produce the approximate operating domain of adverse pressure gradient versus compression ratio shown in Figure 2. The envelope to the domain is controlled therefore by separation, the physical available length of the model, and whether or not the tunnel starting flow can be swallowed by the cowl-centrebody annulus. The pressure gradient parameter β in Figure 2 is a Clauser-type parameter, given as $\beta = (\delta^*/\tau_w)\, dp/dx$ [24], where the boundary layer displacement thickness, δ^*, and wall shear stress, τ_w, are evaluated just upstream of separation. A range of cowls were modelled by CFD, to give an approximate envelope to the operating domain, and four specific designs were subsequently manufactured and tested. The sequence of manufacture and tests was in the order of increasing pressure ratio (and pressure gradient), moving the designs progressively towards the expected limits of flow stalling/flow separation. Figure 3 presents a design sequence for the 7.5:1 pressure ratio, showing the 'target' distribution, plus a three-stage design iteration. The third and final one of these was constructed and the measured test data are included on the figure. This shows a very satisfactory design for a severe pressure gradient case, apart from some difficulty in controlling the initial switch-on of the pressure rise. This is largely associated with the design procedure attempting to 'cancel' the viscous interaction compression wave system radiated from the cowl leading edge.

Two-dimensional laminar cavity flow

The results of this study have been extensively reported in [4], so that only the main points will be referred to here. Cavity flows are of practical interest at hypersonic and at lower speeds. They provide a convenient CFD case since (for rectangular cavities at least) there is the option of using a simple mesh and the separation is more-or-less fixed at the leading edge of the cavity so that mesh refinement requirements can be well-focussed to capture separation correctly.

The configuration used is shown in Figure 4. Several practical design constraints were enforced. *Firstly*, the requirement for flow two-dimensionality automatically implied use of axisymmetric models. *Secondly*, the study was to be laminar and ensuring that laminar flow could be established presented a demanding requirement. A short forebody length was required (we used 200 mm), coupled with testing at our

lowest unit Reynolds number condition. Data clearly confirmed both that the boundary layer at separation was indeed laminar and also that the flow was laminar on the afterbody downstream of the cavity. *Thirdly*, we wished there to be only a minimal pressure gradient imposed by the forebody on the cavity flow itself, so that ideally the forebody should be cylindrical or as close to cylindrical as possible. This automatically means that a *hollow* body of revolution would be required, which then presents a problem of flow starting since there is a maximum permitted 'inlet' area which was then determined by experiment. *Fourthly*, the two main factors that determined the cavity depth were flow establishment times (which was assessed by CFD) and the need for good data resolution. Both of these of course are in conflict, the response time considerations requiring a shallow cavity and the resolution considerations requiring a deep one.

The CFD converged to a *steady* state solution and Figure 5 presents the predicted steady-state streamline pattern for the cavity with a length-to-depth ratio,L/D, of 1.0. It was pointed out [4] that there are close links between this and low speed 'lid-driven' cavity flows. Figure 6 shows comparisons between measurement and computation of heat transfer in the cavity floor, as well as the immediately adjacent segments of the forebody and afterbody. Heat transfer is chosen as the quantity for comparison, since it is a sensitive measure of assessment for CFD codes. Data are presented as a wetted distance, S, along the body surface, referenced to zero at the cavity rear lip, and normalised by the cavity depth, D. Thus the floor of the cavity lies in the range $-2 \leq S/D \leq -1$, and the upstream or 'separation' lip is at $S/D = -3$ and the downstream or 'reattachment' lip is at $S/D = 0$. The experimental data are an accumulation of measurements at four locations around the circumference, clearly showing that axisymmetry of the mean data is established to a high precision. The figure identifies the narrow spike at shear layer impingement ($S/D = 0$), and also the Goldstein-type singularity at the forward 'separation' lip ($S/D = -3$). The only region of discrepancy between experiment and CFD is on the cavity floor however ($-2.0 \leq S/D \leq -1.0$) a difference of more than a 2:1 ratio at the maximum. After elimination of various numerical and experimental possibilities, this difference is now believed to be a consequence of three-dimensional laminar instability in the cavity.

Three-dimensional laminar cavity flows

In the previous section we saw that axisymmetry was established, in the mean, to a very high level of accuracy indeed. A natural way to establish a controlled *three-dimensional* cavity flow therefore was by a *graduated* offset of the afterbody [25], achieved by an eccentric axis arrangement for the afterbody/collar/sting system, so that appropriate rotation enabled it to vary smoothly from axisymmetric to strongly asymmetric. This also means that the minimum amount of instrumentation, usually the most expensive and time-consuming part of model manufacture, can be used to provide a complete effective coverage by relative rotation/movement of modules. Our *initial* modelling (for model design purpose) of the offset case (again the experiments indicated that fully laminar flow is maintained so that the CFD was restricted to laminar modelling) assumed that the flow was 'quasi-two-dimensional', computing a 'local' axisymmetric flow in various azimuthal planes, taking account of the appropriate 'local' changes in afterbody diameter. This is reasonable for the 'weakly' three-dimensional flows, but for strong interactions a full three-dimensional simulation is required. Results of such a full simulation are shown in Figure 7 providing projections of particle paths in various azimuthal planes. This case corresponds to the same cavity length presented in the previous section but now with an offset, d, of 10% of the cavity depth, D. Figure 8 compares CFD and experiment for the azimuthal variation of the

maximum heating on the cavity floor. The very low levels for 180 degrees in azimuth are a consequence of the virtually stagnant flow shown in Figure 7c in contrast to the more vigorous vortex motion in Figure 7a,b.

Unsteady cavity flows

The previous cavity cases that we studied, both two-dimensional axisymmetric and asymmetric, were found to be steady, both in the CFD simulations and in the experiment. Hypersonic cavity flows are not all steady and we have performed combined CFD and experimental studies on a range of cavities that exhibit very significant unsteadiness. The basic test model is a 15 degree semi-angle cone, constructed (on a central sting) in a modular manner, such that modules can be removed to generate annular cavities. A large number of cases have been studied, providing variations in cavity length and depth. The case shown here was selected because we believe that the flow remains laminar and that, although the flow unsteadiness is severe, the flow is also largely axisymmtric; our CFD has been limited to laminar axisymmetric. Figure 9 shows three pictures, representing different stages during the cavity oscillation cycle, with experimental schlieren presented on the top half of each figure and 'computational schlieren' on the bottom.

Three-dimensional turbulent shock-separated boundary layers

From a recent review of shock-wave/boundary-layer interactions [26] it is clear that the number of well-defined three-dimensional interaction studies is still limited, although this really is the case of practical engineering interest. It is in essence this problem that we are beginning to address. Again, therefore, our studies are all configured to provide both a precise two-dimensional (in the mean) reference flow field and also a *controlled* three-dimensional interaction. In the same manner as the offset cavity study, it is intended to provide a *graduated* variation from fully two-dimensional flows, through 'mildly' three-dimensional to 'strongly' three-dimensional. This is intended both to aid the interpretation of flow physics and also to provide a possible bridge between the relative cheapness of two-dimensional CFD simulations and the very considerable effort involved in a full well-resolved simulation of a highly three-dimensional interaction. In each case a hollow cylindrical forebody generates the axisymmetric test boundary layer. A reference axisymmetric separation is then provided either by a concentric cowl (for impinging shock wave separation), or by a concentric flare, both of which can then be offset to produce the three-dimensional flow. Other basic three-dimensional separation studies in the literature include yawed, impinging shock waves or yawed surface-mounted wedges ([27], [28], [29], [30]) and the offset flare configuration has also been utilised elsewhere ([31], [32], [33]). Some results for the offset cowl study have already been reported ([**?**]). As yet our three-dimensional solver is only effectively working for laminar flows, so that configuration development is largely based on prototype tunnel tests. Figure 10, for example, shows schlieren visualisation for an offset flare. Flares can be offset such that their axis is still parallel to that of the forebody ([31], [32], [33]), but for our tests we have pitched a 36 degree semi-vertex angle cone at 4 degrees, to present maximum and minimum deflection angles of 40 degrees (top) and 32 degrees (bottom). Practically, this allows us to minimise the instrumentation, in the same manner as for the 3D cavity flow; the flare is able to rotate around its own axis, whilst keeping the forebody stationary, so that a single stream-wise row of instrumentation along a flare can be used, in successive runs, to provide a full surface coverage. As an interesting preliminary observation we see that, if anything, the total flow separation length on the bottom side is larger than that on the top. From a purely quasi two-dimensional approach,

treating each azimuthal plane as if it were a local axisymmetric configuration, the 40 degrees surface would generate a very substantial separation whereas the 32 degrees surface would essentially be an incipient separation case.

Conclusions

We have presented a range of test problems where there has been a close relationship between CFD and experiment, both in interpreting results and also in the selection and design of the configuration. The increasing cost of experiments, and the reducing costs and increasing accuracy of CFD, means that experiments have to be selected with care so that they provide focussed benchmark test cases.

Acknowledgements

This work has received support from EPSRC and QinetiQ, which is gratefully acknowledged.

References

[1] Rizzi, A.W. and Vos, J.B., "Towards establishing credibility in computational fluid dynamics simulations", AIAA Journal 36, 668-675, 1998.

[2] Oberkampf, W.L., "Design, execution and analysis of validation experiments. Verification and validation in CFD", VKI-lecture series, 2000.

[3] Vos, J.B., Rizzi, A,W. and Darracq, D., "Overview of European validation activities in aeronautics", QNET-CFD Network Newsletter (http://www.qnet-cfd.net):17–20, 2001.

[4] Jackson, A.P., Hillier, R. and Soltani, S., "Experimental and computational study of laminar cavity flows at hypersonic speeds", J Fluid Mech 427, 329-358, 2001.

[5] Hillier, R., Kirk, D. and Soltani, S., "Navier-Stokes computations of hypersonic flows", Int J Num Meth Heat & Fluid Flow 5, 195-211, 1995.

[6] Keyes, F.G., "The heat conductivity, viscosity, specific heat and Prandtl numbers for thirteen gases", Massachussetts Institute of Technology, Project Squid, Tech Report 37, 1952.

[7] Baldwin, B.S. and Lomax, H., "Thin layer approximation and algebraic model for separated turbulent flows", AIAA78-257, 1978.

[8] Menter, F.R., "Eddy viscosity transport equations and their relation to the $k-\epsilon$ model", J Fluids Eng 119, 876-884, 1997.

[9] Patel, V.C., Rodi, W. and Scheurer, G., "Turbulence models for near-wall and low Reynolds number flows: a review", AIAA J 23,1308-1319, 1985.

[10] Wilcox, C.,D., "Turbulence modelling for CFD", DCW Industries, La Canada, California, 1992.

[11] Baldwin, B.S. and Barth, T.J., "A one equation turbulence model for high Reynolds number wall bounded flows", NASA TM102847, 1990.

[12] Goldberg, U.C. and Ramakrishnan, S.V., "A pointwise version of the Baldwin-Barth turbulence model", Int J Comp Fluid Dynamics 1, 321-338, 1994.

[13] Hasan, R.G.M. and McGuirk, J.J., "Assessment of turbulence model performance for transonic flow over an axisymmetric bump", Aero J 105, 17-31, 2001.

[14] Shyy, W. and Krishnamurty, V.S., "Compressibility effects in modeling complex turbulent flows", Prog Aero Sci 33,587–645, 1997.

[15] Mallinson, S.G., Hillier, R., Jackson, A.P., Kirk, D.C., Soltani, S. and Zanchetta, M.A., "Gun tunnel flow calibration: defining input conditions for hypersonic flow computations", Shock Waves 10, 313-322, 2000.

[16] Cook, W.J. and Felderman, E.,J., "Reduction of data from thin-film heat-transfer gauges: a concise numerical technique", AIAA J 4, 561-562, 1966.

[17] Schultz, D.L. and Jones, T.V., "Heat-transfer measurements in short–duration hypersonic facilities", AGARDograph 165, 1973.

[18] Roshko, A. and Thomke, G.J., "Observations of turbulent reattachment behind an axisymmetric downstream-facing step in supersonic flow", AIAA J 4, 975-980, 1966.

[19] Donovan, J.F., Spina, E.F and Smits, A.J., "The structure of a supersonic turbulent boundary layer subjected to concave surface curvature", J Fluid Mech 259, 1-24, 1994.

[20] Kussoy, M.,I., Horstman, C.C. and Acharya, M., "An experimental documentation of pressure gradient and Reynolds number effects on compressible turbulent boundary layers", NASA TM 78488, 1978.

[21] Fernando, E.,M. and Smits, A.,J., "A supersonic turbulent boundary layer in an adverse pressure gradient", J Fluid Mech 211,285-307, 1990.

[22] Smith, D.,R. and Smits, A.,J., "A study of the effects of curvature and compression on the behavior of a supersonic turbulent boundary layer", Experiments in Fluids 18,363-369, 1996.

[23] Mallinson, S.G., Hillier, R. and Jackson, A.P., "Turbulence modelling of hypersonic turbulent boundary layer flows", In Ball, G.J., Hillier, R. and Roberts, G.T., 22nd Int. Symp. on Shock Waves, University of Southampton, pp 1519-1524, 1999.

[24] Laderman, A.J., "Adverse pressure gradient effect on supersonic boundary layer turbulence", AIAA J 18, 1186-1195, 1980.

[25] Jackson, A.P., Hillier, R. and Soltani, S., "A study of two- and three-dimensional separation at hypersonic speeds", In Ball, G.J., Hillier, R. and Roberts, G.T., 22nd Int. Symp. on Shock Waves, University of Southampton, pp 1571-1576, 1999.

[26] Dolling, D.,S., "Fifty years of shock-wave/boundary layer interaction research: What next?", AIAA J 39, 1517-1531, 2001.

[27] Panaras, A.,G., "Review of the physics of swept-shock/boundary layer interactions", Prog Aero Sci 37, 173-244, 1996.

[28] Knight, D.,D., Horstman, C.C. and Bogdonoff, S., "Structure of supersonic turbulent flow past a swept compression corner", AIAA J 30, 890-896, 1992.

[29] Settles, G.S., Horstman, C.C. and McKenzie, T.M., "Experimental and computational study of a swept compression corner interaction flowfield", AIAA J 24, 744-752, 1986.

[30] Kussoy, M.I., Viegas, J.R. and Horstman, C.C., "Investigation of a three-dimensional shock wave separated turbulent boundary layer", AIAA J 18, 1477-1484, 1980.

[31] Brown, J.D., Brown, J.L., Kussoy, M.I., Holt, M. and Horstman, C.C., "Two-component LDV investigation of three-dimensional shock/turbulent boundary-layer interactions", AIAA J 26, 52-56, 1988.

[32] Wideman, J.K., Brown, J.L., Miles, J.B. and Ozcan, O., "Skin-friction measurements in three-dimensional shock-wave/boundary-layer interaction", AIAA J 33, 805-811, 1995.

[33] Gaitonde, D., Shang, J.S. and Edwards, J.R., "Structure of a supersonic three-dimensional/offset-flare turbulent interaction", AIAA J 34, 294-302, 1997.

[34] Boyce, R.R. and Hillier, R., "Shock-induced three-dimensional separation of an axisymmetric hypersonic turbulent boundary layer", AIAA 2000-2226, 2000.

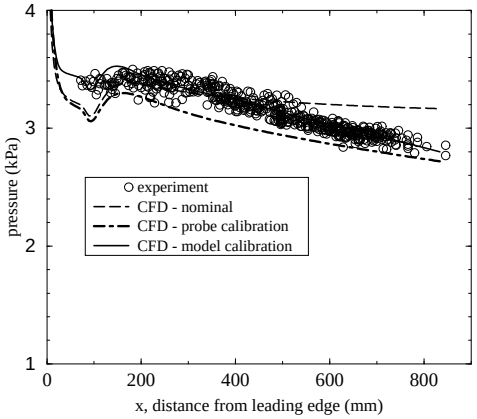

(a) Pressure results

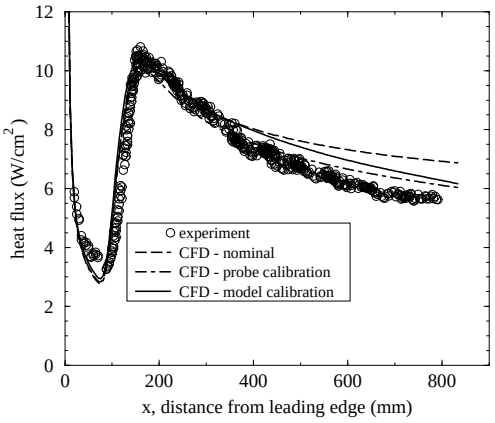

(b) Heat transfer results

Figure 1: Comparison between experiment and CFD for the hollow cylinder model.

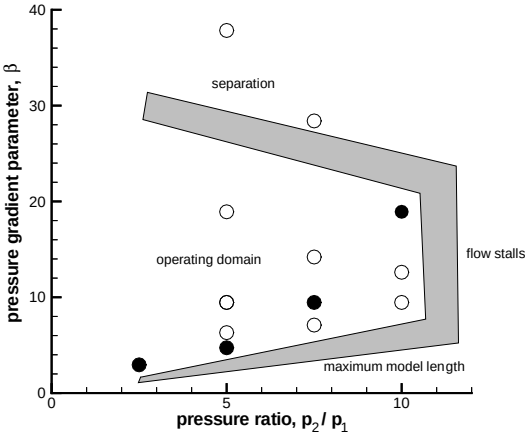

Figure 2: Operating domain for the pressure gradient cowl designs. Open and solid symbols represent CFD simulations; solid symbols represent designs that were subsequently manufactured and tested.

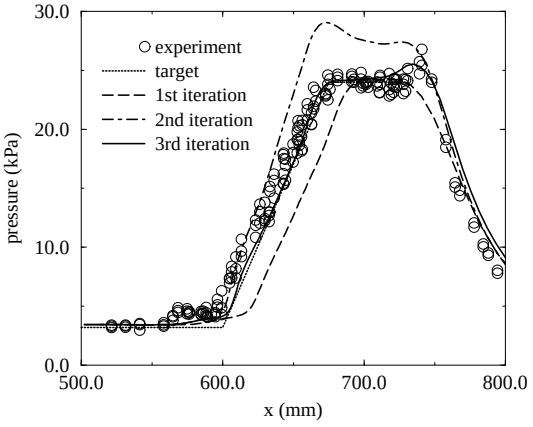

Figure 3: Pressure gradient cowl design. CFD design iterations, and final measured pressure distribution, for 7.5:1 pressure ratio case.

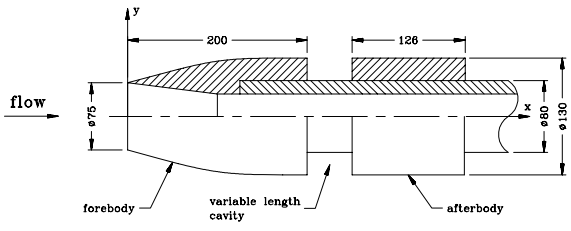

Figure 4: Schematic for the axisymmetric cavity geometry, with dimensions in mm. The cavity depth is 25 mm. and the length is variable.

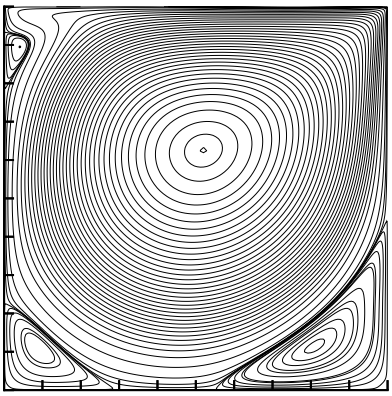

Figure 5: Axisymmetric cavity with length-to-depth ratio, L/D, of 1.0 showing predicted streamlines

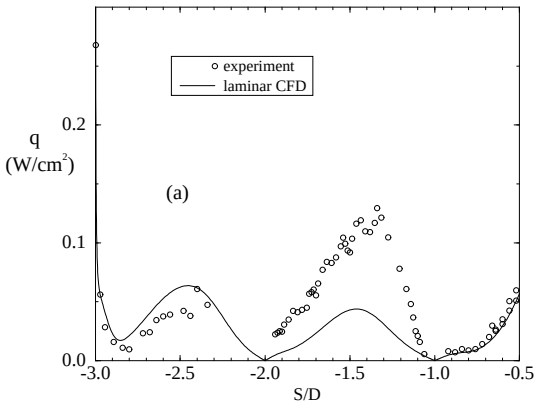

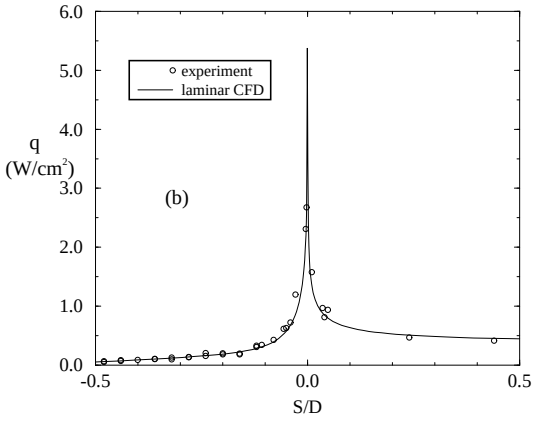

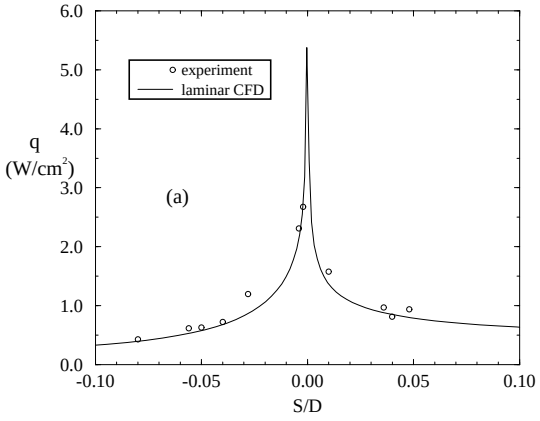

Figure 6: CFD and experiment for the cavity with L/D = 1.

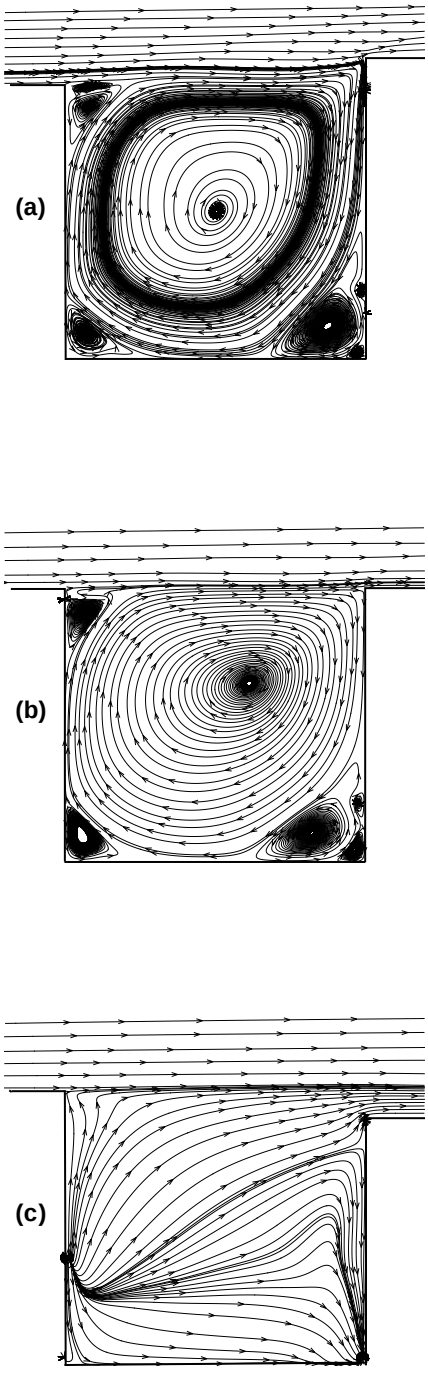

Figure 7: Particle paths for the offset cavity. (a) 0 degrees, (b) 90 degrees and (c) 180 degrees in azimuth

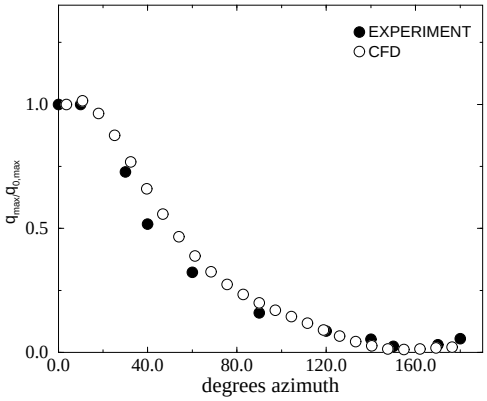

Figure 8: Three-dimensional cavity. Variation of maximum heat transfer on the cavity floor with azimuthal angle

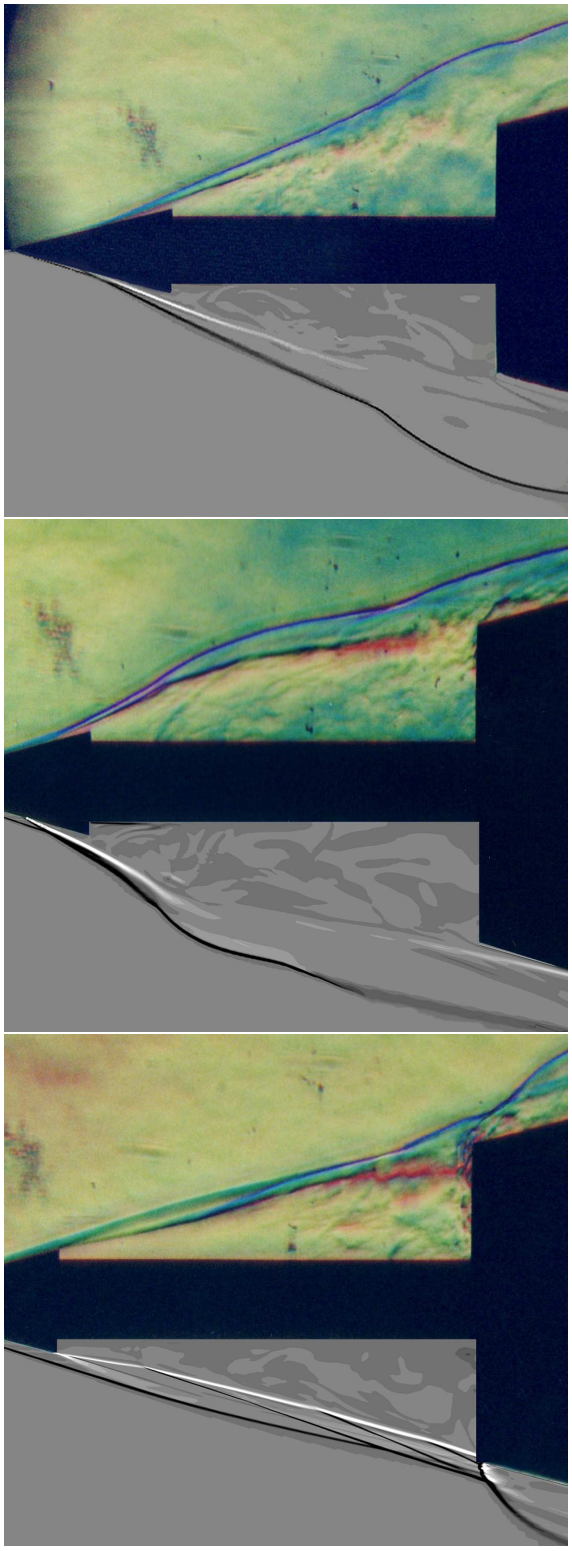

Figure 9: Unsteady cavity flow on body of revolution. Comparison between experimental (top half) and CFD schlieren (bottom half)

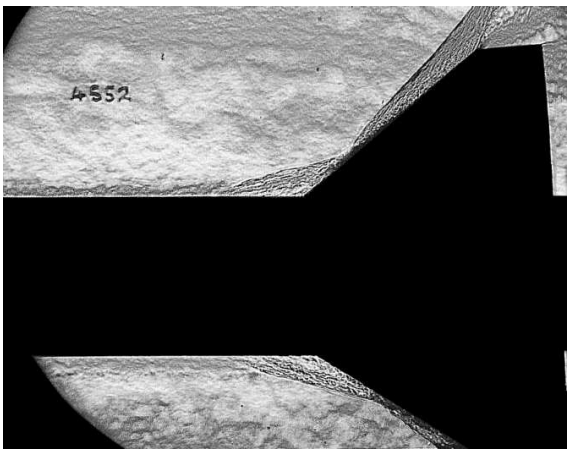

Figure 10: Schlieren for offset flare configuration. Forebody diameter is 75 mm; the flare semi-angle is 36 degrees and the flare axis is pitched at 4 degrees